A 2-1/2 Dimensional Model of Miram Curves*

Abhijit Jassem[1], David P. Chernin[2], Serguei Ovtchinnikov[2], John J. Petillo[2], Yue Ying Lau[1*]

[1]University of Michigan, Ann Arbor, MI 48109, USA
[2]Leidos, Inc., USA
*yylau@umich.edu

Abstract: *This paper reports recent developments of a semi-analytic 2-1/2D model which could provide a realistic description of the Miram curves. We solve the Vlasov and Poisson equations in 3-dimensions assuming an infinite magnetic field, but include electron thermal emission and non-uniform distribution of work function on the cathode surface. This 2-1/2 D theory will be compared with 3D MICHELLE runs.*

Keywords: Cathode, Miram curve, space charge limited, thermionic emission, work function;

The anode current vs. the cathode temperature characteristic of a diode using a thermionic cathode is commonly known as the Miram [1] or 'rollover' curve, and the transition from temperature to space charge limited flow is referred to as the 'knee' in the curve. This transition is very abrupt in a 1D model, that is, the knee is very sharp. In measurements, however, the transition is generally found to be significantly more gradual than in 1D theory

The physical reasons behind the shape of Miram curves have been a mystery for decades, despite significant efforts to analyze them, both in experiments and in modeling. This is an important matter because a thermionic cathode is almost always operated in the vicinity of the knee in linear beam tubes, due to considerations of thermal stability and long cathode life.

We recently used the MICHELLE simulation code, and a novel analytical "1-1/2D model", to examine the knee on the Miram curves [2]. We reached the following conclusions: (a) electron thermal motion parallel to the cathode surface is not the major cause for the smoothness of the knee on the Miram curve, (b) the non-emitting region, because it does not provide space-charge shielding, enables its neighboring low-work function region to yield an anode current density that exceeds the 1D Child-Langmuir prediction, especially near the boundaries between the non-emitting and emitting regions and, therefore, (c) even with a sizeable non-emitting region, the anode current is still governed by the 1D Child-Langmuir law, as if the entire cathode surface were emitting.

These results were obtained from the 1-1/2D model, where the electron motion is limited to 1D by assuming an infinite magnetic field B_z, but the potential is solved for in 2D, allowing the local work function $\phi(y)$ to vary in the y-direction on the cathode surface which lies in the x-y plane. When the distribution of the work function assumes a few (~4 or 5) discrete values spatially, including a very large value to represent a non-emitting stripe in y, the 1-1/2 D model yields a Miram curve which exhibits 4 or 5 different slopes. The different slopes on a Miram curve were also revealed in MICHELLE when there is a similar spatial distribution of discrete work functions in y. MICHELLE further showed that the resulting Miram curves are virtually independent of the value of Bz used in the simulations [2]. However, if similar spatial variations of the discrete work function distributions are also allowed in the x-direction on the cathode surface, the 3D MICHELLE code simulations show a very smooth and rounded Miram curve, much like those experimentally observed [2]. It is therefore of substantial interest to extend the 1-1/2D model to 2-1/2D, allowing the local work function $\phi(x, y)$ to vary in both x and y directions on the cathode surface. The versatility of the 2-1/2D code may definitively answer whether the smoothness and roundedness observed in Miram curves is due mainly to the 2D effects in the work function distribution, or in large part due to the presence of significant non-emitting regions on the cathode .

For the 2-1/2D model, we consider a simple planar diode with the grounded cathode located at $z = 0$ and the anode at voltage V_A at $z = d$. An infinite magnetic field B_z is imposed. Allowing for local variations in the work function, the emitted current density at the cathode is given by the Richardson-Dushman equation:

$$J_{RD}(x, y) = AT^2 e^{-\phi(x,y)/kT} \tag{1}$$

where A is the Richardson coefficient, T is the cathode temperature, and $\phi(x, y)$ is the local work function. Following the approach of Fry and Langmuir [3,4], we construct the following electron distribution function as a solution of Vlasov's equation,

$$f(x, y, z, v_z) = \frac{J_{RD}(x, y)}{v_{th}^2} \exp\left(-\frac{mv_z^2/2 + qV(x, y, z)}{kT}\right) \tag{2}$$

Poisson's equation may be written:

$$\nabla^2 V(x, y, z) = \frac{1}{\epsilon_0 v_{th}} \sqrt{\frac{\pi}{2}} J_{RD}(x, y) e^{-qV(x,y,z)/kT} erfc\left(\frac{v_{min}(x, y, z)}{\sqrt{2} v_{th}}\right) \tag{3}$$

where ϵ_0 is the permittivity of free space, $v_{th} = \sqrt{kT/m}$ is the thermal velocity, $v_{min}(x, y, z)$ is the minimum value of velocity of any electron originated from (x,y) can reach location z to the anode. For $\phi(x, y)$ to be periodic functions of (x, y) with periods p_x and p_y, an iterative algorithm was developed to solve a discretized version of (3). Since the electron motion is limited to 1D but the potential is solved for in 3D, we call this the "2-1/2D model". [2]

We define N_x and N_y 'cell centered' values of x and y respectively as

$$x_i = \frac{i+1/2}{N_x}\frac{p_x}{2} \quad (4)$$

$$y_j = \frac{j+1/2}{N_y}\frac{p_y}{2} \quad (5)$$

for $i = 0,1,2,\dots,N_x - 1$and $j = 0,1,2,\dots,N_y - 1$. We then express the potential as a Fourier series:

$$V_{ij}(z) = \frac{4}{N_x N_y}\sum_{l=0}^{N_x-1}{}'\sum_{m=0}^{N_y-1}{}'\tilde{V}_{lm}(z)\cos\left(\frac{2\pi l x_i}{p_x}\right)\cos\left(\frac{2\pi m y_j}{p_y}\right) \quad (6)$$

for $l = 0,1,2,\dots,N_x - 1$ and $m = 0,1,2,\dots,N_y - 1$ where the prime marks on the summations mean that the $l = 0, m = 0$ terms each have an additional factor of ½. We may then discretize the second derivatives of x and y in (3) and reduce the 3D problem to a set of coupled 1D problems to find that $\tilde{V}_{lm}(z)$ satisfies

$$\frac{d^2}{dz^2}\tilde{V}_{lm}(z) - 2\left[\frac{1-\cos\theta_l}{\Delta x^2} + \frac{1-\cos\theta_m}{\Delta y^2}\right]\tilde{V}_{lm}(z) = \tilde{S}_{lm}(x,y,z) \quad (7)$$

where $\theta_l = \frac{\pi l}{N_x}$ and $\theta_m = \frac{\pi m}{N_y}$, and $\tilde{S}_{lm}(x,y,z)$ is the Fourier transform of S_{ij}, which is the right hand side of (3):

$$\tilde{S}_{lm} = \sum_{i=0}^{N_x-1}\sum_{j=0}^{N_y-1} S_{ij}\cos\left(\frac{2\pi l x_i}{p_x}\right)\cos\left(\frac{2\pi m y_j}{p_y}\right) \quad (8)$$

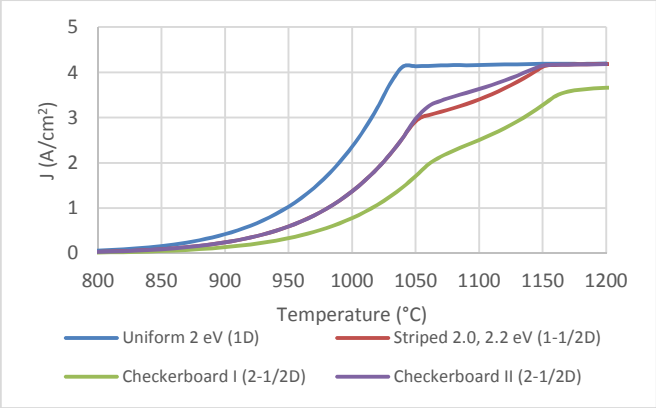

Figure 1. Miram curves for different work function distributions

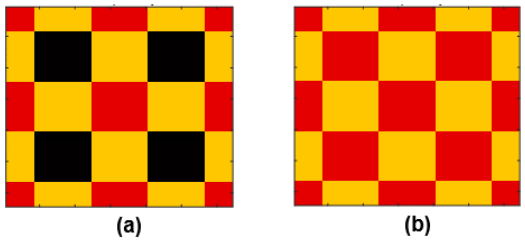

Figure 2. Cathode work function distributions for (a) Checkerboard I, (b) Checkerboard II. Red tiles represent 2.0 eV, orange tiles represent 2.2 eV and black tiles represent 10 eV

The required boundary conditions on $\tilde{V}_{lm}(z)$ are:

$$\tilde{V}_{lm}(0) = 0 \quad (9a)$$

$$\tilde{V}_{lm}(d) = N_x N_y V_a \text{ for } l = 0 \,\&\, m = 0$$
$$\tilde{V}_{lm}(d) = 0 \text{ otherwise} \quad (9b)$$

We begin with an approximate solution for the potential which we denote as $V_{ij}^{(n)}(z)$ where the superscript (n) denotes the n-th approximation in our iterative solution [2]. We then evaluate $S_{ij}(x,y,z)$ by computing the right hand side of (3), which requires finding the potential minimum of $V_{ij}^{(n)}(z)$. We then compute the Fourier coefficients of $\tilde{S}_{lm}$ using (8), solve (7) for $\tilde{V}_{lm}(z)$ subject to the boundary conditions in (9) and transform the solution to $V_{ij}(z)$ using (6). We call this $V_{ij}^{(n+)}(z)$ and instead define the next iteration of the potential as

$$V_{ij}^{(n+1)}(z) = \alpha V_{ij}^{(n)}(z) + (1-\alpha)V_{ij}^{(n+)}(z) \quad (10)$$

where the mixing parameter α is a real number satisfying $0 < \alpha < 1$. The value of α must be obtained empirically, but were typically set in a range from 0.8-1. We iterate this algorithm until the solution converges everywhere to 1 part in 10^4.

Fig. 1 shows preliminary results of the above 2-1/2D code, setting $V_A = 179.5$ V and $d = 0.381$ mm [2]. The blue curve recovers the 1D results [3,4] with a uniform work function 2.0 eV, and the red curve recovers the 1-1/2D results [2] with alternate stripes (in y) of work functions 2.0 and 2.2 eV and 265μm width. The green and purple curves show the 2-1/2D results with $\phi(x,y)$ given by the two checkerboard patterns shown in Fig. 2, setting the tile width to 265μm. These novel 2-1/2D results will be tested against results from 3D MICHELLE, in which a large axial magnetic field is applied. Eventually, realistic work function distributions obtained from experiments, will be implemented in the 2-1/2D model, and the results will be compared with the corresponding 3D MICHELLE simulations and with experimental measurements.

** This research was developed with funding from the Defense Advanced Research Projects Agency (DARPA). The views, opinions and/or findings expressed are those of the authors and should not be interpreted as representing the official views or policies of the Department of Defense or the U.S. Government.*

References

1. M. Cattelino, G. Miram and W. Ayers, "A diagnostic technique for evaluation of cathode emission performance and defects in vehicle assembly," in *IEDM Technical Digest,* San Francisco, 1982.
2. D. Chernin,. Y. Y. Lau, J. J. Petillo , S. Ovtchinnikov, D. Chen, A. Jassem, R. Jacobs, D. Morgan, J. Booske, "Effect of non-uniform emission on Miram curves," *IEEE Trans. Plasma. Sci* [accepted for publication.]
3. T. Fry, "The thermionic current between parallel plane electrodes; velocities of emission distributed according to Maxwell's law," *Phys. Rev.,* vol. 17, p. 441, 1921.
4. I. Langmuir, "The effect of space charge and initial velocities on the potential distribution and thermionic current between parallel plates," *Phys. Rev.,* vol. 21, p.419,1923